멤브레인(Membrane Journal)
Vol. 26 No. 6 December, 2016, 480-489

Print ISSN: 1226-0088
Online ISSN: 2288-7253
DOI: https://doi.org/10.14579/MEMBRANE_JOURNAL.2016.26.6.480

전기방사법을 이용한 PVdF/Fe_3O_4-GO(MGO) 복합 분리막 제조 및 비소 제거 특성평가

장 원 기 · 후 건 · 변 홍 식 · 이 재 용*,†

계명대학교 화학공학과, *(주)케이엠

(2016년 12월 20일 접수, 2016년 12월 28일 수정, 2016년 12월 29일 채택)

Preparation of PVdF/Fe_3O_4-GO (MGO) Composite Membrane by Using Electrospinning Technology and its Arsenic Removal Characteristics

Wongi Jang, Jian Hou, Hongsik Byun, and Jae Yong Lee*,†

Department of Chemical Engineering, Keimyung University, Daegu 42601, Republic of Korea
*KM Corp., 727 Seounro, Miyang, Anseong, Gyeonggi 17599, Republic of Korea

(Received December 20, 2016, Revised December 28, 2016, Accepted December 29, 2016)

요 약: 본 연구에서는, 전기방사법을 이용하여 산화철-산화그래핀(Fe_3O_4/GO, metallic graphene oxide; MGO)이 도입된 PVdF/MGO 복합나노섬유(PMG)를 제조하였으며, 이를 활용하여 비소제거에 대한 특성 평가를 진행하였다. MGO의 경우 In-situ-wet chemical 방법으로 제조하였으며, FT-IR, XRD분석을 진행하여, 형태와 구조를 확인하였다. 나노섬유 분리막의 기계적 강도 개선을 위하여 열처리과정을 진행하였으며, 제조된 분리막의 우수한 기계적 강도 개선 효과를 확인할 수 있었다. 그러나, PMG 막의 경우, 도입된 MGO의 함량이 증가할수록 기계적 강도가 감소되는 경향성을 보여주었으며, 기공크기 분석 결과로부터, 0.3~0.45 μm의 기공크기를 가진 다공성 분리막이 제조되었음을 확인할 수 있었다. 수처리용 분리막으로의 활용 가능성 조사를 위해, 수투과도 분석을 실시하였다. 특히, PMG2.0 샘플의 경우 0.3 bar 조건에서, PVdF 나노섬유막(91 kg/m^2h)에 비해 약 70% 향상된 결과값(153 kg/m^2h)을 나타내었다. 또한, 비소 흡착실험 결과로부터, PMG 막의 경우, 비소3가와 5가에 최대 81%, 68%의 높은 제거율을 보여주었으며, 흡착등온선 분석으로부터, 제조된 PMG 막의 경우 비소3가, 5가 모두 Freundlich 흡착거동을 따른다는 것을 확인하였다. 위 모든 결과로부터, PVdF/MGO 복합 나노섬유 분리막은 비소제거 및 수처리용 분리막으로 충분히 활용할 수 있을 것으로 판단된다.

Abstract: In this study, the PVdF/MGO composite nanofiber membranes (PMGs) introducing Iron oxide-Graphene oxide (Fe_3O_4/GO, Metallic graphene oxide; MGO) was prepared via electrospinng method and its arsenic removal characteristics were investigated. The thermal treatment was carried out to improve the mechanical strength of nanofiber membranes and then the results showed that of outstanding improvement effect. However, in case of PMGs, the decreasing tendency of mechanical strength was indicated as increasing MGO contents. From the results of pore-size analysis, it was confirmed that the porous structured membranes with 0.3 to 0.45 μm were prepared. For the water treatment application, the water flux measurement was carried out. In particular, PMG2.0 sample showed about 70% improved water flux results (153 kg/m^2h) compared to that of pure PVdF nanofiber membrane (91 kg/m^2h) under the 0.3 bar condition. In addition, the PMGs have indicated the high removal rates of both As(III) and As(V) (up to 81% and 68%, respectively). Based on the adsorption isotherm analysis, the adsorption of As(III) and As(V) ions were both more suitable for the Freundlich. From all of results, it was concluded that PVdF/MGO composite nanofiber membranes could be utilized as a water treatment membrane and for the Arsenic removal applications.

***Keywords**: Fe_3O_4-GO, Functionalized graphene oxide, Arsenic removal, Electrospinning, Nanofiber membrane*

†Corresponding author(e-mail: dragonlee@kmbiz.com, http://orcid.org/0000-0001-8771-3203)

1. Introduction

Water pollution due to toxic heavy metals caused by industries and agricultural sources is one of the most serious environmental and public problems[1,2]. Arsenic is a ubiquitous, toxic and carcinogenic chemical element among these heavy metals. However, arsenic is infamous for its marked negative impacts on human health because it's chronic and carcinogenic effects as well as acute lethality. Inorganic arsenic species, arsenate (As(V)) and arsenite (As(III)), are believed to be more toxic than the organic forms. As(V) is predominate in surface waters, while As(III) is dominant in groundwater systems. Drinking water contamination by arsenic remains a major public health problem around the world, especially in India, USA, China, Vietnam, etc. Therefore, it is highly desired to develop eco-friendly, simple and economical techniques for arsenic removal[3].

As arsenic contamination is a widespread problem, many methods have been developed to remove arsenic such as adsorption[4-6], ion exchange[7], membrane separation[8,9], chemical oxidation[10], bioremediation [11], and so on. Among these techniques, the adsorption and the membrane separation processes are more cost-effective and simple to operate, so they have played very important roles in the water purification industry[12,13].

Up to now a lot of absorbents have been reported for arsenic water removal, including nano-scale metal oxide[14], activated carbons and graphene derivatives [15,16]. Among these adsorbents, iron oxides, such as Fe_2O_3 and Fe_3O_4, are promising efficient adsorbents for arsenic because of its large active surface area and high arsenic adsorption capacity. However it cannot be applied in the continuous flow systems due to its small particles size and the aggregation effect. Consequently, it is necessary to load iron oxide onto an appropriate support such as the activated carbon[17].

Recently, Graphene Oxide (GO) has received intensive attentions due to its high surface area (2,630 m^2/g) and chemical stability. In addition, as the GO has many negative functional groups including hydroxyl, carboxyl, and carbonyl group, it can be used as a great adsorbent for heavy metal removal from polluted and other natural water resources. However, some reviews on the use of GO-based materials as a support to load iron oxide for the removal of arsenic in water is available[18,19]. In specific, the reviews on the membrane application have not been extensively studied or published.

Electrospinning is a simple and versatile method for fabricating continuous fibers with diameters ranging from micrometers to several nanometers[20,21]. High specific surface area with excellent adsorption capacity can be obtained by electrospinning[22]. So here we reported on our work to prepare PVdF/MGO composite membranes via an electrospinning technique and the resulting composite nanofiber membranes were characterized for their arsenic adsorption ability for the wastewater treatment.

2. Experimental

2.1. Materials

Graphite flake (SP-1, Bay city Inc.), sulfuric acid (≥ 98%, Duksan Pure Chemical Co. Ltd), potassium permanganate (≥ 99.9%, Sigma Aldrich), hydrogen peroxide (35%, Samchen Co. Ltd), $FeCl_3 \cdot 6H_2O$ (≥ 97.0%, Sigma Aldrich), $FeCl_2 \cdot 4H_2O$ (≥ 99.0%, Samchun Chemical) and hydrochloric acid (1N, Duksan Pure Chemical Co. Ltd.) were used to synthetize MGO.

PVdF (Kynar 761, Arkema), N,N-dimethyl acetamide (DMAc) (≥ 99.0%, Duksan Pure Chemical Co. Ltd.), acetone (≥ 99.0%, Duksan Pure Chemical Co. Ltd.) were used to prepare PVdF nanofiber.

As(III) standard solution (1,000 ± 3 ppm) and As(V) standard solution (1,000 ± 3 ppm) were purchased from Sigma Aldrich. The distilled water (DI water) was purified through a Millipore system (~18 MΩ · cm). All of the chemicals and reagents were used without further purification.

Table 1. Composition of Electrospinning Solutions

Sample code	PVdF (wt%)	MGO (wt%)	DMAc (wt%)	Acetone (wt%)
PVdF	15	0.0	68	17
PMG 2.0	15	2.0	68	17
PMG 3.0	15	3.0	68	17
PMG 4.0	15	4.0	68	17

2.2. Synthesis of GO and Fe_3O_4-GO (M-GO)

GO and MGO were synthesized using the Hummer's method through oxidation of graphite flake and the detailed procedure was previously reported[23,24]. The GO nanosheets were obtained by filtering GO solution dispersed 1 mg/mL of density with a vacuum filtration system using a 0.45 μm PVdF filter (Millipore Co., Ltd.). To prepare MGO composites, 0.1 g of GO nanosheets were completely dispersed in 100 mL DI water by sonication. Then, the solution was transferred to a three-neck flask and purged with N_2 for 5 min in order to remove dissolved oxygen. A mixed solution of $FeCl_3 \cdot 6H_2O$ dissolved in DI water and $FeCl_2 \cdot 4H_2O$ dissolved in HCl were taken into the GO solution slowly. The mixture was stirred for 15 min. After that NH_4OH was added to the mixture and stirred for 45 min. The reaction processed under the protection of N_2. The products were collected by vacuum filtration and washed several times with ethanol and DI water. The resulting black solids were vacuum-dried at 70 °C for 2 h. Finally, the obtained black powders were stored in a N_2-purged desiccator.

2.3. Preparation of PVdF/MGO composite nanofiber membrane

For preparation of PVdF/MGO composite nanofiber membrane, the different concentrations of MGO (2.0-4.0 wt%) was initially dispersed in a DMAc by sonication for 2 h. Then, the PVdF powder and acetone were added to the MGO solutions and were stirred for overnight at room temperature. The composition of elelctrospinning solutions is listed in Table 1. Then, the PVdF/MGO solution was loaded into the 5 mL of plastic syringe equipped with a syringe needle. After that, the electrosinning was performed with following conditions; an applied voltage of 15 kV, a tip-collector distance of 15 cm, at a flow rate of 0.6 mL/h, an aluminum foil collector. Finally, the collected nanofibers were thermally treated at 120°C for 24 h after stacking it's layers between glass plates. The layered composite nanofiber membrane was used for further characterization.

2.4. Characterization of synthesized MGO and composite nanofiber membranes

2.4.1. Morphology and structure analysis

FT-IR (Thermo Scientific, IS50) spectroscopy was used to characterize the functional groups of MGO. The crystallographic structures of MGO were characterized with X-ray diffraction (XRD) patterns on a Rigaku D, Max-2500V with nickel-filtered Cu Kα radiation. The surface morphology of composite nanofiber membranes were determined using STEM (S-4800, Hitach) after osmium coating.

2.4.2. Mechanical strength and pore-property measurements

The tensile strength of composite nanofiber membranes were obtained using a universal testing machine (UTM-2020, MYUNGJI TECH). The mechanical test was performed according to ASTM D882. The samples were cut in a rectangular shape with dimension of 100 mm × 20 mm and directly mounted on the sample clamps at a rate of 500 mm/min. The tensile-test results were obtained by averaging the data of five measurements for each sample.

The pore size of the composite nanofiber membranes were measured by the Capillary Flow Porometer (Porolux 1000, Porous Materials Inc.) with Porewick solution (16.0 dynes/cm) and then the effective diameter of

sample was fixed at 1.9 cm. The porosity of the composite nanofiber membranes were measured using the n-butanol uptake test. The porosity was calculated as:

$$\text{Porosity}\,\% = \frac{W_{wet} - W_{dry}}{\rho_b V_{dry}} \times 100\% \quad (1)$$

Where W_{dry} and W_{wet} are the weights of the composite membranes before dry and after socking (wet) in n-butanol for 2 h, ρ_b is the density of n-butanol, and V_{dry} is the volume of the dry membranes. The composite membranes were cut into squares of 16.0 cm^2 (4 cm × 4 cm) for the tests.

2.4.3. Contact angle analysis and pure water permeate measurement

The wettability of the composite nanofiber membranes were observed with water droplet placed on their surfaces and confirmed by a contact angle analyzer (Phoenix 300, SEO). The final contact angles were obtained as the average of five measurements at room temperature.

A dead-end cell was used for pure water flux measurement[23]. The membrane active area was 38.5 cm^2. The feed solution was stirred at a rate of 200 rpm. The filtrate was collected over a given period and weighed. The flux was calculated from the equation:

$$\text{Water flux}\,(kg/m^2 \cdot h) = m_x/A_x \cdot \triangle t \quad (2)$$

Where m_x is the weight of the filtrate (kg), t is the filtration time (h), and A_x is effective area of membrane (m^2).

2.4.4. Arsenic adsorption measurement

Two well-known adsorption isotherms namely Langmuir and Freundlich are widely used to investigate the equilibrium data of As(III) and As(V) ions. The general form of the Langmuir isotherm is:

$$\frac{C_e}{q_e} = \frac{1}{q_m} C_e + \frac{1}{q_m \cdot b} \quad (3)$$

Where C_e (mg/L) is the equilibrium concentration of the adsorbent, q_e (mg/g) is the mass of adsorbate adsorbed per mass of adsorbent, q_m (mg/g) is the maximum adsorption capacity of adsorbent and b (L/mg) is constant which is related to the absorption rate. The values of q_m and b are calculated by plotting C_e/q_e versus C_e, respectively.

The Freundlich expression is commonly presented as follows:

$$\text{In}q_e = \text{In}K_F + \left(\frac{1}{n}\right)\text{In}C_e \quad (4)$$

Where K_F and n are the Freundlich constants related to the adsorption capacity and intensity of the sorbent, respectively.

The concentration of arsenic ions in the adsorption by the composite nanofiber membrane was determined using an inductively coupled plasma atomic emission spectrophotometer (ICP, Optima 7300 DV, Perkin-Elmer). The removal rate was calculated by:

$$R(\%) = \left(\frac{C_i - C_f}{C_i}\right) \times 100 \quad (5)$$

Where R is removal rate of arsenic ions (%), C_i and C_f are before and after concentration of arsenic ion solutions, respectively.

3. Results and Discussion

3.1. Morphology and structure analysis

FT-IR spectra of GO and MGO nanocomposites are shown in Fig. 1. Several characteristic peaks of GO can be observed, confirming the successful formation of GO. Absorption peaks appearing at 1,040, 1,740, 1,620 and 3,400 cm^{-1} in the FTIR spectra of GO are attributed to O-C-O group, C=O group, C=C group, and -OH group, respectively. However, that of MGO wasn't observed at 1,740 cm^{-1} attributed to carboxylic group (-COOH). It could be explained that the GO was partially reduced during synthesis procedure with Fe_3O_4,

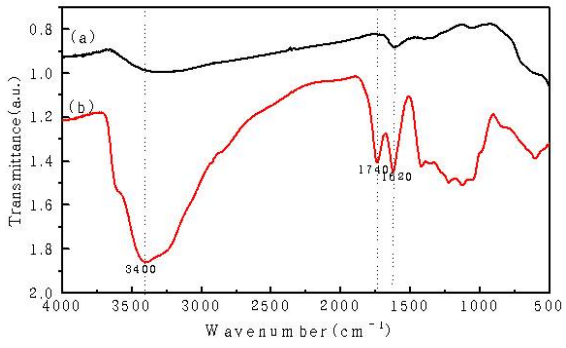

Fig. 1. FT-IR spectra of (a) MGO and (b) GO.

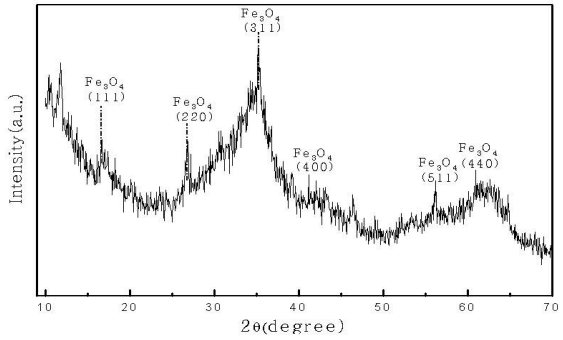

Fig. 2. XRD pattern of MGO.

thus, it is expected that wettability of MGO could be lower than that of GO.

The crystalline structures of MGO were identified with XRD. The XRD pattern of MGO is shown in Fig. 2. Six diffraction lines can be observed at 2θ = 17.50, 27.10, 35.50, 42.25, 56.75 and 61.50°. These diffraction lines can be assigned to the (111), (220), (311), (400), (511) and (440) crystalline planes of Fe_3O_4[25]. This confirmed that MGO was successfully synthesized with Fe_3O_4.

Fig. 3 shows the SEM images of PVdF nanofiber membrane and prepared composite nanofiber membranes under magnification of 5,000 x. The diameters of PVdF and PMG nanofibers ranged between 500 and 1500 nm. Then some heterogeneous components above the composite nanofiber membranes were observed, which was ascribed to the agglomeration of PVdF polymer and MGO nanocomposites (Fig. 3 b-d). It might be concluded that the porosity of PMGs was decreased due to the agglomeration of PVdF and MGO resulting in the blocking of the pores.

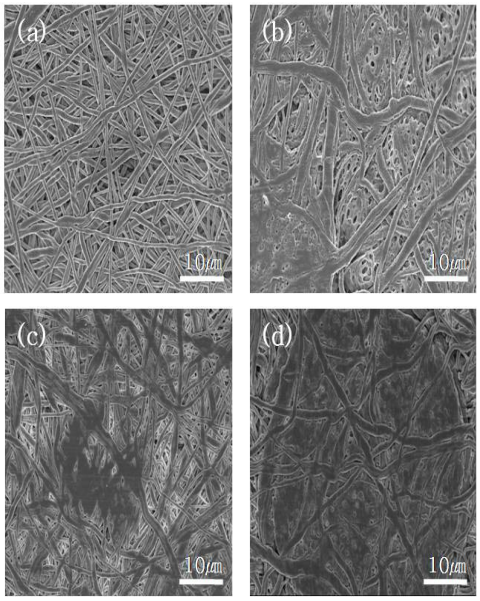

Fig. 3. SEM image of PVdF and PMG nanofiber membranes; (a) PVdF nanofiber membrane (b) PMG 2.0 (c) PMG 3.0, and (d) PMG 4.0 (5,000 x, white bar = 10 μm).

3.2. Mechanical strength and pore property measurements

The tensile strength was measured as mechanical property of prepared nanofiber membranes. That of nanofiber membranes with and without MGO are summarized in Table 2. The pure PVdF nanofiber membrane showed the highest tensile strength and elongation values (283.7 kgf/cm^2, 114.8%). In case of PMGs, the tensile strength gradually decreased with increasing MGO contents in nanofiber membrane and the value of elongation was similarly indicated at all of PMGs. In our previous study[23] and several researches[26], it was reported that the mechanical strength of hybrid or composite membranes was enhanced with introducing GO contents due to a strong hydrogen bond interaction between the GO and polymer matrix. However, the MGO is appearing the metallic and partially reduced structures, thus, it is difficult to form the chemical bond between the MGO and polymer matrix. In this study, the thermal treatment was performed at high temperature to improve the mechanical strength and then physical bonds was formed in the nanofiber itself because the nanofiber was slightly melted at this

Table 2. Tensile Strength and Elongation of Nanofiber Membranes

Sample code	PVdF	PMG 2.0	PMG 3.0	PMG 4.0
Tensile strength (kgf/cm^2)	283.7 ± 11.4	103.6 ± 5.4	84.5 ± 6.2	41.9 ± 4.2
Elongation (%)	114.8 ± 11.0	51.6 ± 3.2	51.0 ± 2.5	59.3 ± 4.1

Table 3. Pore-Properties of Nanofiber Membranes

Sample code	Bubble point (μm)	Avg. pore diameter (μm)	Smallest pore diameter (μm)	Porosity (%)	Thickness (μm)
PVdF	0.373 ± 0.002	0.300 ± 0.016	0.294 ± 0.012	25.60 ± 2.12	45-55
PMG 2.0	0.647 ± 0.003	0.458 ± 0.034	0.214 ± 0.060	20.17 ± 1.16	46-51
PMG 3.0	0.592 ± 0.031	0.418 ± 0.036	0.275 ± 0.063	18.51 ± 1.41	50-53
PMG 4.0	0.506 ± 0.009	0.315 ± 0.001	0.280 ± 0.033	13.23 ± 1.01	55-58

procedure. However, in case of PMGs, it is speculated that physical bond formation in the nanofiber itself has been interrupted by positioning the MGO having thermal stability between the nanofibers. Thus, it was expected that the tensile strength and elongation values of PMGs was indicated to lower than that of pure PVdF nanofiber membranes.

The pore diameter and porosity of nanofiber membranes can be controlled by different contents of MGO. The results are summarized in Table 3. The pore size appeared the increasing tendency with the increase of MGO. However, the bubble point increased firstly and then decreased with the adding of MGO. As the composite membranes contain more than a certain amount of MGO, the excess MGO could fill the empty space of the pore and be responsible for the decrease in bubble point. For the same reason, the porosity of composite membranes showed the similar tendency.

3.3. Contact angle analysis and pure water permeate measurement

The surface energy for a membrane is analogous to the surface tension of a liquid and usually measured by indirect methods such as direct force measurements, contact angles, and capillary penetration[27]. Then the contact angle reflects the relative strength of the liquid, solid, and vapor molecular interaction. Young's equation can be determined to the three surface tension values of the system: the solid-liquid surface tension (γ sl), the solid-vapor surface tension (γ sv), and the liquid-vapor surface tension(γ lv). Young's equation can be given by:

$$\gamma \mathrm{lv} \cos\theta = \gamma sv - \gamma sl \quad (6)$$

Where θ is the contact angle between the solid and the liquid. Based on this principle, it can be concluded to the lower contact angle, the lower surface energy of the membrane.

The contact angle results of prepared nanofiber membranes are shown in Fig. 4. That values gradually decreased from 80° to 42° with the increase of MGO contents in the PVdF nanofiber membranes. Based on this results, it was expected that the water permeability of PMGs could be improved than that of PVdF nanofiber membranes because the low energy membranes can give higher liquid permeation rates.

Fig. 5 shows the pure water flux of prepared nanofiber membranes. Based on the contact angle results (Fig. 4), the water flux of the PMG composite membranes increased against the PVdF nanofiber membranes due to its lower surface energy and increased pore diameter (Table 3). In particular, the PMG 2.0 composite nanofiber membrane showed 70% improved values (153 kg/m^{2}h) of water flux than that of PVdF nanofiber membrane (91 kg/m^{2}h) at 0.3 bar. In case of PMG 4.0 samples, the pore diameter (0.315 μm) was similar to that of PVdF nanofiber membranes (0.3

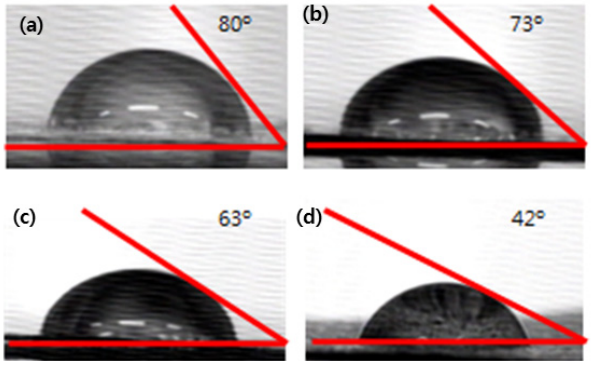

Fig. 4. Contact angle of nanofiber membranes; (a) PVdF nanofiber membrane (b) PMG 2.0, (c) PMG 3.0, and (d) PMG 4.0.

μm), then the porosity (13%) was very lower than that of PVdF (25%). However, it was confirmed that the water-flux values (115 kg/m^{2}h) of PMG 4.0 increased compared to that of PVdF (91 kg/m^{2}h) under 0.3 bar condition. Based on overall results, the permeate property of PVdF nanofiber membranes could be improved by the proper addition of MGO contents.

3.4. Arsenic adsorption measurement

The adsorption rate of As(III) and As(V) for prepared nanofiber membranes were investigated. The adsorption test was confirmed by a batch test using 100 mL stock solution (0.1 mg/g of As(III) and As(V) ions in pure water). The membrane (8 cm × 8 cm) were placed in an incubator and then shaken for 24 hours at room temperature to completely react with metal ions. After collecting the supernatant, the adsorption rate was investigated with before and after concentration of arsenic solutions. The results were shown in Fig. 6. The PVdF nanofiber membrane showed no adsorption effect for both As(III) and As(V) ions. However, the PMG membranes have shown good adsorption rate with the increase of MGO content. The removal rate of As(III) increased from 74% to 81% and that of As(V) increased from 57% to 68% as a function of MGO content in the PVdF nanofiber membranes.

The isotherm models of Langmuir and Freundlich were applied to fit the adsorption equilibrium data of As(III) and As(V) on the PMGs. The results of adsorption isotherms were listed in Fig. 7 and Table 4 was listed the relative parameters calculated from Langmuir and Freundlich models. The adsorption of As(III) and As(V) were both more suitable for the Freundlich model with higher R^2 (0.9878 and 0.9616, respectively). According to the K_F values, the adsorption of As(III) was higher than As(V). Based on these models, the maximum amount of metal ions adsorbed per unit weight of PMGs (q_m) was calculated to be at 0.72 mg/g of As(III) and 0.31 mg/g of As(V), respectively. From these results, it was speculated that PMG have more adsorption effect for As(III) compared to As(V).

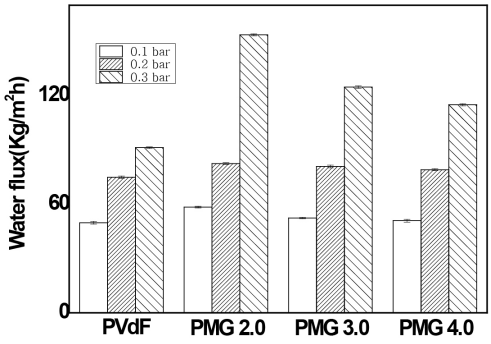

Fig. 5. Water flux of nanofiber membranes at 0.1, 0.2, 0.3 bar and room temperature.

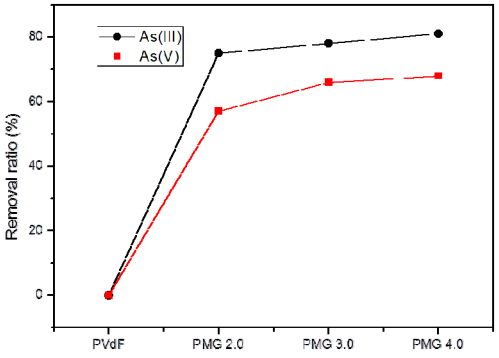

Fig. 6. Removal rate of As(III) and As(V) for composite nanofiber membranes with 100 mL stock solution (0.1 mg/g) at pH 7 and room temperature.

4. Conclusions

In this study, the nanocomposites of MGO were successfully synthesized and confirmed with the results of

Table 4. Parameters for Langmuir and Freundlich Models of As(III) and As(V) by MGO

	Langmuir			Freundlich		
heavy-metal ion	q_m (mg/g)	b (L/mg)	R^2	K_F	1/n	R^2
As(III)	0.72	1.12	0.8850	0.42	0.74	0.9878
As(V)	0.31	1.73	0.7950	0.20	0.53	0.9616

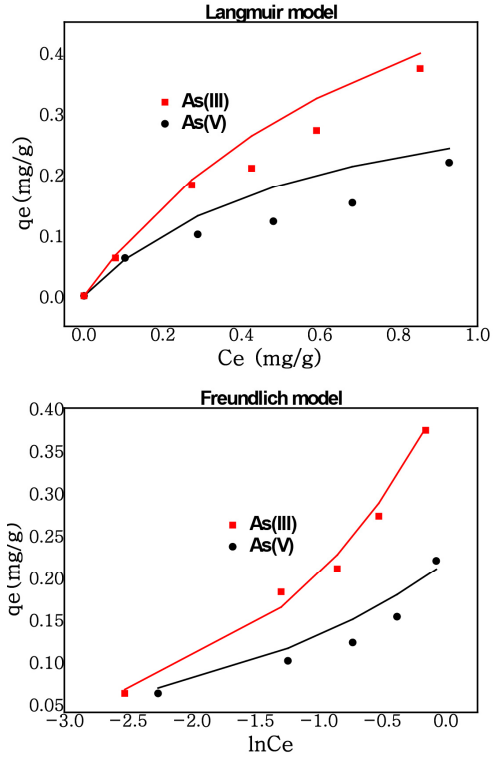

Fig. 7. Langmuir and Freundlich adsorption isotherm as a function of As(III) and As(V) concentration (0.1 mg/L) with PMG 2.0 sample at pH 7 and room temperature.

SEM, FT-IR, XRD analysis. The PVdF/ MGO composite nanofiber membrane (PMG) was prepared by electrospinning technique and investigated as an adsorbent for the removal of arsenic ions from the water. It was shown that the mechanical property of PVdF nanofiber membranes was improved by thermal treatment. In case of PMGs, the tensile strength gradually decreased with increasing MGO contents in nanofiber membrane and the value of elongation was not much different at all of PMGs. The pore diameter was controlled for 0.45 to 0.3 μm with MGO contents. The contact angle of the PMGs decreased from 80° to 42° with the increase of MGO contents. The PMG 2.0 composite nanofiber membrane showed 70% improved water-flux values (153 kg/m^2h) compared to that of PVdF nanofiber membrane (91 kg/m^2h) at 0.3 bar. In case of PMG 4.0 samples, the pore-diameter (0.315 μm) was similar to that of PVdF nanofiber membranes (0.3 μm), then the porosity (13%) was very lower than that of PVdF (25%). However, it was confirmed that the water-flux values (115 kg/m^2h) of PMG 4.0 increased compared to that of PVdF (91 kg/m^2h) under 0.3 bar condition. In addition, the PMG membranes showed the high removal rates of both As(III) and As(V) (up to 81% and 68%, respectively). Based on the adsorption isotherm analysis for arsenic ions, the adsorption of As(III) and As(V) ions were both more suitable for the Freundlich model with higher R^2 (0.9878 and 0.9616, respectively). From all of results, it was concluded that PVdF/MGO composite nanofiber membranes could be a good candidate for the removal of arsenic ions, i.e. As(III) and As(V), in wastewater treatment.

Acknowledgement

This work was supported by the Korea Institute of Energy Technology Evaluation and Planing (KETEP) grant funded by the Korea government (MOTIE) (No. 20152010103210).

Reference

1. M. J. Gonzalez-Munoz, M. A. Rodriguez, S. Luque, and J. R. Alvarez, “Recovery of heavy metals from metal industry waste waters by chemical precipitation and nanofiltration”, *Desalination*, **200**, 742 (2006).

2. Y. J. Kim, S. J. Park, and M. Kim, "Capture of metal ions by corss-linked sulfonic acid type ion exchange membrane", *Membr. J.*, **19**, 333 (2009).
3. X. Luo, C. Wang, S. Luo, R. Dong, X. Tu, and G. Zeng, "Adsorption of As(III) and As(V) from water using magnetite Fe_3O_4-reduced graphite oxide-MnO_2 nanocomposites", *Chem. Eng. J.*, **187**, 45 (2012).
4. A. Sperlich, A. Werner, A. Genz, G. Amy, E. Worch, and M. Jekel, "Breakthrough behavior of granular ferric hydroxide (GFH) fixed-bed adsorption filters: modeling and experimental approaches", *Water Res.*, **39**, 1190 (2005).
5. Q. L. Zhang, Y. C. Lin, X. Chen, and N. Y. Gao, "A method for preparing ferric activated carbon composites adsorbents to remove arsenic from drinking water", *J. Hazard. Mater.*, **148**, 671 (2007).
6. K. J. Reddy, K. J. McDonald, and H. King, "A novel arsenic removal process for water using cupric oxide nanoparticles", *J. Colloid. Interface Sci.*, **397**, 96 (2013).
7. J. S. Kim and M. M. Benjamin, "Modeling a novel ion exchange process for arsenic and nitrate removal", *Water Res.*, **38**, 2053 (2004).
8. R. Y. Ning, "Arsenic removal by reverse osmosis", Desalination, **143**(3), 237 (2002).
9. G. Borbely and E. Nagy, "Removal of zinc and nickel ions by complexation-membrane filtration process from industrial wastewater", *Desalination*, **240**, 218 (2009).
10. A. Heidari, H. Younesi, and Z. Mehraban, "Removal of Ni(II), Cd(II), and Pb(II) from a ternary aqueous solution by amino functionalized mesoporous and nano mesoporous silica", *Chem. Eng. J.*, **153**, 70 (2009).
11. E. O. Omoregie, R. M. Couture, P. V. Cappellen, C. L. Corkhill, J. M. Charnock, D. A. Polya, D. Vaughan, K. Vanbroekhoven, and J. R. Lloyd, "Arsenic bioremediation by biogenic iron oxides and sulfides", *Appl. Environ. Microbiol.*, **79**, 4325 (2013).
12. C. H. Lee, C. L. Chiang, and S. J. Liu, "Electrospun nanofibrous rhodanine/polymethylmethacrylate membranes for the removal of heavy metal ions", *Sep. Purif. Technol.*, **118**, 737 (2013).
13. M. Hua, S. Zhang, B. Pan, W. Zhangm, L. Lv, and Q. Zahng, "Heavy metal removal from water/wastewater by nanosized metal oxides: A review", *J. Hazard. Mater.*, **211-212**, 317 (2012).
14. B. Manna and U. C. Ghosh, "Adsorption of arsenic from aqueous solution on synthetic hydrous stannic oxide", *J. Hazar. Mater.*, **144**, 522 (2007).
15. L. Lorenzen, J. S. J. V. Deventer, and W. M. Landi, "Factors affecting the mechanism of the adsorption of arsenic species on activated carbon", *Miner. Eng.*, **8**, 557 (1995).
16. T. N. Narayanan, Z. Liu, P. R. Lakshmy, W. Gao, Y. Nagaoka, D. S. Kumar, J. Lou, R. Vajtai, and P. M. Ajayan, "Synthesis of reduced grapheme oxide-Fe_3O_4 multifunctional freestanding membranes and their temperature dependent electronic transport properties", *Carbon*, **50**, 1338 (2012).
17. C. Wang, H. Luo, Z. Zhang, Y. Wu, J. Zhang, and S. Chen, "Removal of As(III) and As(V) from aqueous solutions using nanoscale zero valent iron-reduced graphite oxide modified composites", *J. Hazard. Mater.*, **268**, 124 (2014).
18. L. Guo, P. Ye, J. Wang, F. Fu, and Z. Wu, "Three-dimensional Fe_3O_4-graphene macroscopic composites for arsenic and arsenate removal", *J. Hazard. Mater.*, **298**, 28 (2015).
19. L. Li, G. Zhou, Z. Weng, X. Y. Shan, F. Li, and H. M. Cheng, "Monolithic Fe_2O_3/graphene hybrid for highly efficient lithium storage and arsenic removal", *Carbon*, **67**, 500 (2014).
20. H. D. Lee, Y. H. Cho, and H. B. Park, "Current research trends in water treatment membranes based on nano materials and nano technologies", *Membr. J.*, **23**, 101 (2013).
21. T. H. Kim, "Current R&D trend of nanofiber membranes", *Membr. J.*, **22**, 395 (2012).
22. Y. Tian, M. Wu, R. Liu, Y. Li, D. Wang, J. Tan,

R. Wu, and Y. Huang, "Electrospun membrane of cellulose acetate for heavy metal ion adsorption in water treatment", *Carbohydr. Polym.*, **83**, 743 (2011).

23. W. G. Jang, J. H. Yun, K. S. Jeon, and H. S. Byun, "PVdF/graphene oxide hybrid membranes via electrospinning for water treatment applications", *RSC Adv.*, **5**, 46711 (2015).
24. W. G. Jang, J, H. Yun, and H. S. Byun, "Preparation of PAN nanofiber composite membrane with Fe_3O_4 functionalized graphene oxide and its application as a water treatment membrane", *Membr. J.*, **24**, 151 (2014).
25. Y. Song, Z. He, H. Hou, X. Wang, and L. wang, "Architecture of Fe_3O_4-graphene oxide nanocomposite and its application as a platform for amino acid biosensing", *Electrochim. Acta*, **71**, 58 (2012).
26. J. W. Lee, H. R. Chae, Y. J. Won, K. B. Lee, C. H. Lee, H. H. Lee, I. C. Kim, and J. M. Lee, "Graphene oxide nanoplatelets composite membrane with hydrophilic and antifouling properties for wastewater treatment", *J. Membr. Sci.*, **448**, 223 (2013).
27. D. Bhanushali, S. Kloos, C. Kurth, and D. Bhattacharyya, "Performance of solvent-resistant membranes for non-aqueous system: solvent permeation results and modeling", *J. Membr. Sci.*, **189**, 1 (2001).